Journal of Ultrafine Grained and Nanostructured Materials
https://jufgnsm.ut.ac.ir
Vol. 51, No.1, June 2018, pp. 90-95
Print ISSN: 2423-6845 Online ISSN: 2423-6837
DOI: 10.22059/JUFGNSM.2018.01.12

Effect of hydrolysis rate on the properties of TiO_2-CNT nanocomposite powder prepared by sol-gel method

Alireza Shafei[1], Saeed Sheibani*[*,1]

[1]School of Metallurgy and Materials Engineering, College of Engineering, University of Tehran, Tehran, Iran.

Recieved: 22 October 2017; Accepted: 1 March 2018

** Corresponding author email: ssheibani@ut.ac.ir*

ABSTRACT

In this study, TiO_2-10%wt. carbon nanotube (CNT) nanocomposite powders were synthesized by sol-gel method at various hydrolysis rate affected by different reaction agents of acetyl acetone and benzyl alcohol. Crystallization of TiO_2 was then achieved through calcination at 400 °C. The properties of nanocomposite powder investigated by scanning electron microscopy, X-ray diffraction and diffuse reflectance spectroscopy. The results showed that, the crystalline TiO_2 with anatase structure was produced after calcination. The crystallite size of TiO_2 depended on the hydrolysis rate which was increased from 25 nm at higher hydrolysis rate by benzyl alcohol to 55 nm at slower hydrolysis rate by acetyl acetone. Before calcination, the results have shown that the slower hydrolysis rate yields relatively large particles with a plate like morphology in contrast to the presence of small particles with significant agglomeration at higher hydrolysis rate by benzyl alcohol. After calcination, high hydrolysis reaction through the use of benzyl alcohol offers easy access to the TiO_2-10%wt. CNT nanocomposite with well controlled coating and desirable interactions between TiO_2 and the CNTs. The thickness of TiO_2 coating on CNTs in this way was 80 nm. Also, TiO_2 particle size depended on the hydrolysis rate, decreased from 1 µm in presence of acetyl acetone to 150 nm in presence of benzyl alcohol. The band gap energy at higher hydrolysis rate by benzyl alcohol was 2.95 eV.

Keywords: *Nanocomposite; Carbon nanotube; TiO2; Sol-gel; Hydrolysis rate.*

1. Introduction

The area of heterogeneous photocatalysis is a rapidly expanding technology for water and air treatment. Among the semiconductor photocatalyst materials, TiO_2 remains a most popular candidate in environmental cleaning due to its high catalytic activity, chemical stability in aqueous media and low cost [1]. However, TiO_2 can only absorb the ultraviolet region of solar spectrum due to its large band gap. Hence, it is essential to extend the light absorption of it to the visible region. Also, it suffers in fast electron-hole pair recombination [2]. These problems can be solved by several approaches such as optimization of particles morphology, metal doping of TiO_2 and fabrication of composite photocatalyst [3]. In recent years, the combination of carbon nanotubes with TiO_2 photocatalyst has been attracting increasing attention as a possible strategy [4-8]. Carbon-related materials have been extensively studied [9] for the catalytic applications either by serving as a supporting matrix to tailor the electronic or photonic properties of catalysts, or as catalyst by itself. Particularly, CNTs can act as the scaffolds to anchor light harvesting assemblies, due to their unique electrical and electronic properties, wide electrochemical stability and high surface area [10-12]. Therefore, their advantageous structural features to extend the light response range and

other distinctive features, such as facile charge separation, and increased adsorption of pollutants are the reason for combination of CNTs with TiO_2 photocatalyst [13,14].

TiO_2-CNT nanocomposites have been synthesized recently by different chemical routes, such as sol-gel and hydrothermal methods [15,16]. The sol-gel method is one of the most common methods used to synthesize TiO_2-CNT nanocomposites [8,17-18]. The main advantage of this method is low temperature processing of homogeneous oxides in various forms and compositions [19]. However, difference in synthesis parameters of sol-gel process affects the morphology of TiO_2-CNT nanocomposites significantly [16,20]. On the other hand, the photocatalytic performance of TiO_2-CNT nanocomposite depends on its morphology which can be determined by preparation condition. In this work TiO_2-10%wt. CNT nanocomposite powder is prepared by the sol-gel method. The main focus is on the structure and morphology of nanocomposite powder before and after calcination step investigated by scanning electron microscopy (SEM) and X-ray diffraction (XRD) analysis. Also, the optical properties were evaluated by diffuse reflectance spectroscopy (DRS). The aim of the present study is to investigate the influence of hydrolysis rate by different reaction agents of acetyl acetone and benzyl alcohol on the structure and morphology of the powder. Actually, the morphology and hence the optical properties of synthesized TiO_2-10wt.% CNT powders were compared in details.

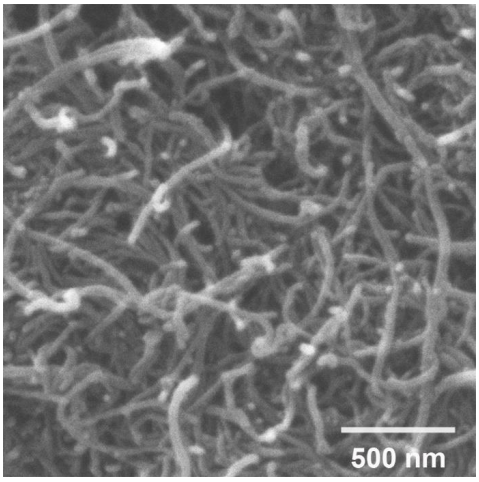

Fig. 1- SEM image of the initial functionalized CNT.

2. Experimental procedure

The starting materials used in this work were tetrabutyl-orthotitanate (TBOT) as a precursor, ethanol (EtOH) as a solvent, deionized water for hydrolysis, acetyl acetone (AcAc) as a chelating agent, benzyl alcohol (BA) as a surfactant. Also, multi-walled CNT (~10 μm in length) with a purity of about 98% were used. CNTs were chemically functionalized by ultrasonication in a mixture of sulfuric acid and nitric acid (3:1) for 8 h. The SEM image of the initial CNTs was shown in Fig. 1.

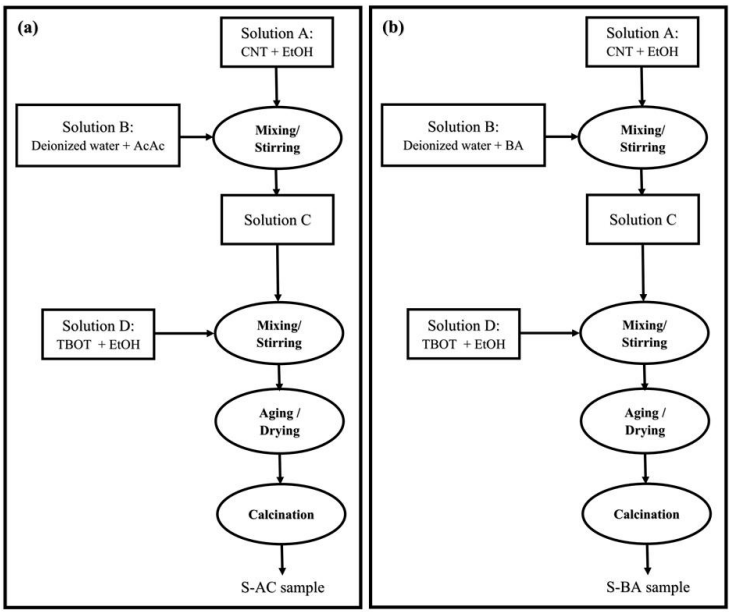

Fig. 2- Flow chart of synthesis process for (a) S-AC and (b) S-BA samples.

Using the Imagej software, the average diameter of CNT was obtained 40 nm.

The flow chart of synthesis process for the TiO_2-10%wt. CNT nanocomposite is shown in Fig. 2. During synthesis, two different but equal parts of ethanol solutions were prepared. The solution A was prepared by dispersion of an appropriate amount of CNTs in EtOH with the aid of ultrasonication for 10 minutes. In order to investigate the effect of AcAc and BA in the preparation of TiO_2-CNT nanocomposite powder, the hydrolysis solution B was prepared by mixing deionized water with AcAc (Fig. 2 (a)) or BA (Fig.2 (b)). These two solutions were then mixed to obtain solution C and the solution kept stirring at 0 ˚C. In addition, the solution D was then prepared by dissolution of TBOT into EtOH. Then solution D was added drop by drop into solution C under vigorous stirring and additionally stirred for 1 h. The final molar ratio of a mixture of TBOT: AcAc or BA: EtOH: H_2O was 1: 5: 100: 5. Slow hydrolysis reaction occurred with the presence of AcAc agent (here after called S-AC sample). Hence after aging at room temperature for 24 h, the sample was dried at 80 °C for 48 h. On the other hand, rapid hydrolysis occurred when BA surfactant was used (here after called S-BA sample) and the precipitates were vacuum-filtered, washed in ethanol and dried at room temperature for 24 h. Finally in a calcination step, both samples heat treated at 400 °C for 2 h.

The morphological study was performed by a Hitachi S4160 SEM. The Ultraviolet-visible (UV-Vis) spectra of the samples were recorded by diffuse reflectance spectroscopy (DRS, Shimadzu, MPC-2200). The spectral absorbance was measured in the wavelength range of 200-800 nm. XRD using Philips PW3040/60 diffractometer with Cu-K_α radiation were used for the structural characterization. The average crystallite size of the samples was calculated by the Scherrer equation [21]:

$$d = k\lambda/(\beta \cos(\theta)) \quad \text{(eq. 1)}$$

where, d is the crystallite size, k is a coefficient (0.89), λ is the wavelength of the Cu K_α radiation, β is the full width at half maximum and θ is the scattering angle.

3. Results and Discussion

To characterize the crystal structure of the calcined samples, XRD analysis was carried out on S-AC and S-BA nanocomposite samples. The XRD patterns of both samples after calcination in Fig. 3 revealed clear peaks which can be indexed to pure anatase TiO_2 phase (JCPDS Card No. 21-1272). Also, the peaks at 2θ values of 26°, 43.4° were associated with the (002) and (101) diffractions of the CNTs (JCPDS Card No. 75-1621). It should be noted, the (101) reflection of TiO_2 overlap with (002) reflection of CNT at 2θ=26°. However, 10wt.%CNT was high enough to clearly observe the main peaks in XRD pattern. The observed peaks positions are in complete accordance with those reported in previous studies for TiO_2-CNTs composites powders [8, 22-24]. In addition, the oxidation temperature of CNT is above 500 ° C [8]. It should be noted that no other diffraction peaks corresponding to other phase of TiO_2 i.e. rutile and brookite or any crystalline impurity were observed from the XRD patterns. The predominant existence of pure anatase phase TiO_2 and the absence of the rutile phase was beneficial to the photocatalytic activity of the composite catalysts, owing to higher photocatalytic activity of anatase than that of rutile [25]. Furthermore, this both samples exhibited quite similar XRD diffraction patterns. However, the crystallite size of TiO_2 in S-AC and S-BA samples calculated by Scherrer equation were 55 and 25 nm, respectively. It is observed that the increase of hydrolysis rate using BA in the initial solution of preparation procedure resulted in a significant decrease in the crystallite size of TiO_2.

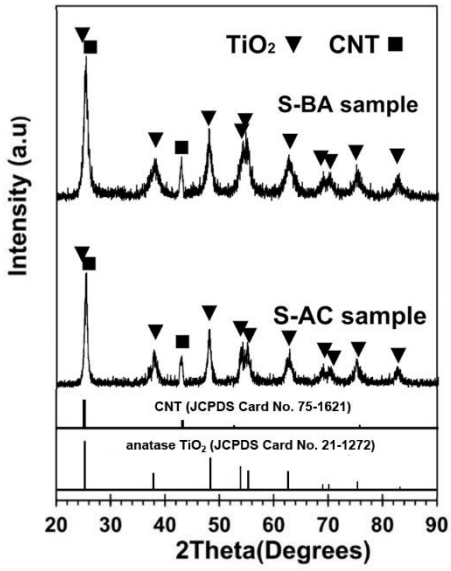

Fig. 3- XRD patterns of S-AC and S-BA samples after calcination.

The reason for this result is interactions of BA's benzene ring to enable the use of CNTs [8] and thus reduce the crystallite size.

The morphology of the as-prepared TiO_2-10wt.% CNT nanocomposite powders before calcination were further characterized by SEM (Fig. 4). Depending on the hydrolysis rate, microstructure of the as-prepared samples is completely different. Regarding relatively large and plate-like particles of S-AC sample in Fig. 4 (a), no formation of loose particle with the typical shape was evidenced at slow hydrolysis reaction. Slow rate of hydrolysis by AcAc leads the gel structure can be influenced and get into a glassy plate-like powder. This is due to different reactivity of the chelate complexes, such as AcAc, depending on the type and number of bidentate ligands [26]. Furthermore, Fig. 4 (a) indicates uniformly distributed CNTs in the microstructure. Fig. 4 (b) shows the SEM images of as-prepared precipitates in S-BA sample. This reveals the TiO_2 agglomerates growth selectively on the CNTs at higher hydrolysis rate by hydroxyl group of OH in BA agent. In the first step of reaction, the hydroxyl group generates Ti-OH groups which provides the TiO_2 condensation on CNT or elsewhere [27].

Fig. 5 shows the morphology of the TiO_2-10wt.% CNT nanocomposite powders after calcination. After calcination, the difference of S-AC sample morphology in Fig. 5 (a) compared to Fig. 4 (a) is significant. Freely growth of large TiO_2 particles together with CNTs can be seen at low hydrolysis rate by addition of AcAc. In sharp contrast, at higher hydrolysis rate by BA addition, it seems that the surface of CNTs is covered with TiO_2 (showed by white arrows in Fig. 5 (b)). Using the Imagej software, the average diameter of these CNTs was obtained 120 nm. In comparison to the initial CNTs diameter, it means that, the average thickness of TiO_2 layer on CNTs is approximately 80 nm. Although TiO_2 agglomerates can be seen in the SEM image probably due to the low specific surface area, the TiO_2 particles are more distributed between the CNTs. This leads to more desirable interaction

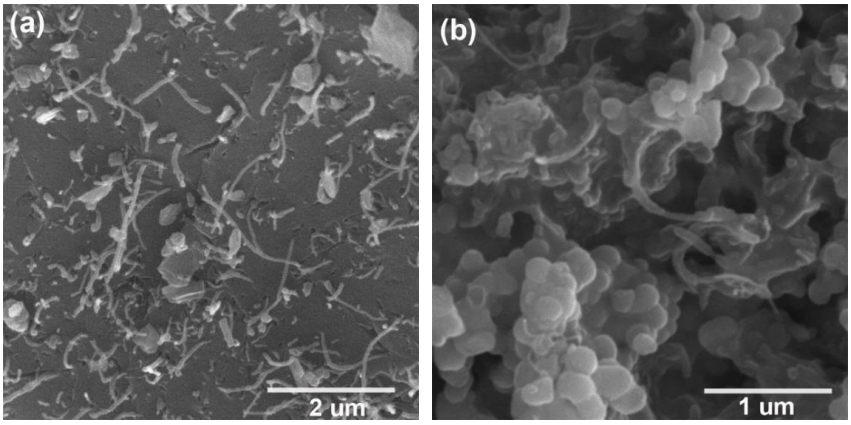

Fig. 4- SEM images of (a) S-AC and (b) S-BA samples before calcination.

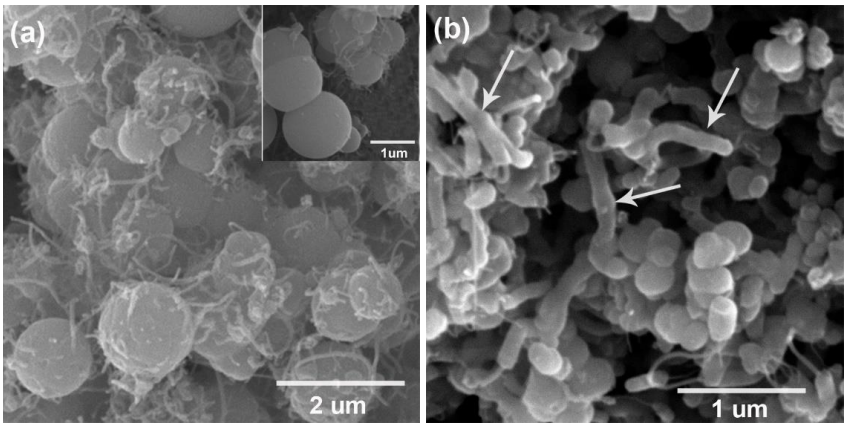

Fig. 5- SEM images of (a) S-AC and (b) S-BA samples after calcination.

between both components of the composites. In addition, the average particles size of TiO_2 depends on the hydrolysis rate. Using the ImageJ software, the average TiO_2 particles size was measured. It can be found that the TiO_2 particle size decreased from 1 μm in presence of AcAc (in Fig. 5 (a)) to 150 nm in presence of BA (in Fig. 5 (b)). The main reason is possibly that the BA adsorbs on the surface of CNTs via π-π interactions, while at the same time providing hydrophilic hydroxyl groups for the hydrolysis of the Ti precursor. Hence, despite their hydrophobic surface, CNTs can indeed be used as a template. Then, the dispersion of CNTs could be significantly improved with the addition of BA and better coating was provided on the surface of CNT [17]. This is in complete agreement with the smaller crystallite size at higher hydrolysis rate by BA addition from XRD results.

The optical properties were examined by DRS to calculate the band gap energies of samples. Fig. 6 represents the UV-vis DRS of the S-AC and S-BA samples. It can clearly be seen that, both samples exhibited an absorption in the visible range (>400 nm). The results clearly show the difference between two samples. The band gap energies (E_g) were estimated using the following equation [28].

$$(\alpha h\upsilon)^2 = d(h\upsilon - E_g) \quad \text{(eq. 2)}$$

where α is the absorption coefficient, d is a proportional constant, h is the Planck's constant, ν is the frequency of vibration and hν is the energy of incident photons. The usual method for determining E_g involves plotting $(\alpha h\upsilon)^2$ against hν (Tauc plot). Tauc plots of S-AC and S-BA samples are shown in Fig. 6 (b). Hence, the optical band gap for the absorption peak can be obtained by extrapolating the linear portion of the curve. The approximate band gap energies of S-AC and S-BA samples are 3.17 and 2.95 eV, respectively. This shift showed that the E_g of the S-BA sample was decreased gradually. This effect is probably due to the better chemical interaction between CNT and TiO_2 in S-BA sample, as mentioned above, to reduce the band gap energy. Another possible reason for the large band gap change from S-AC to S-BA samples may be due to the organic residues in the latter sample. Totally, an increase in light absorption is favorable as light absorption is one of the critical factors for a photocalayst.

4. Conclusions

TiO_2-10%wt. CNT nanocomposite powder was successfully prepared by sol-gel method. The main intention was to investigate the effect of hydrolysis rate on the structure and morphology through the addition of two different types of agents, AcAc and BA. The results are summarized as follows:

1. TiO_2 anatase phase was the main crystalline phase present after calcination of nanocomposite powder. The increase of hydrolysis rate using BA in the initial solution resulted in a significant decrease in the crystallite size of TiO_2 from 55 to 25 nm.

2. Before calcination, relatively large and plate-like particles with uniformly distributed CNTs were prepared in presence of AcAc at slow hydrolysis reaction. In comparison, smaller TiO_2 agglomerates formed selectively on the CNTs at higher hydrolysis rate by BA agent.

3. After calcination, relatively large TiO_2 particles and CNTs can be formed at low hydrolysis rate by addition of AcAc. At higher hydrolysis rate by BA

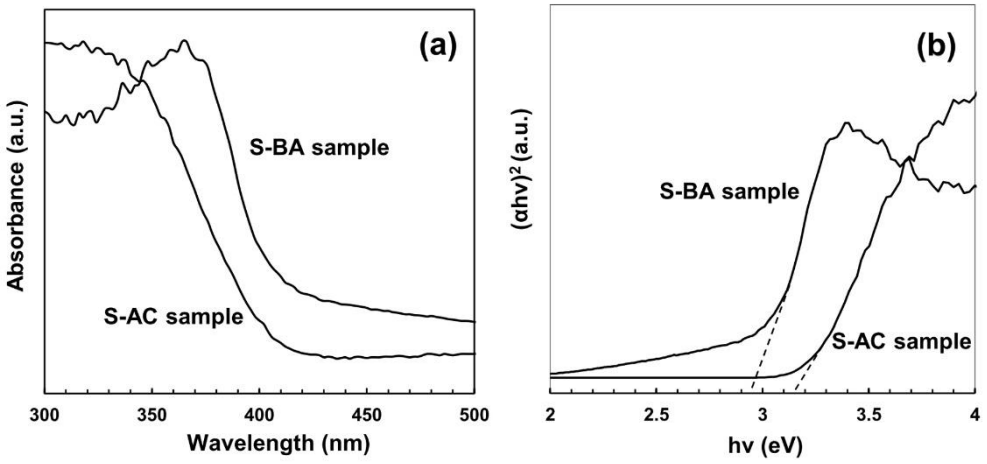

Fig. 6- (a) UV-Vis absorption spectra of S-AC and S-BA samples and (b) corresponding Tauc plots of samples.

addition, covered CNTs by TiO_2 with the average thickness of 80 nm together with more distributed TiO_2 particles were obtained.

4. Depending upon the hydrolysis rate in the first step of reaction, the average particles size of TiO_2 decreased from 1 μm in presence of AcAc to 150 nm in presence of BA.

5. The band gap energy decreased gradually from 3.17 to 2.95 eV with the increase of hydrolysis rate by BA addition.

5. Acknowledgments

The authors would like to acknowledge the financial support of University of Tehran for this research. Also, financial support of Iran Nanotechnology Initiative Council is gratefully acknowledged.

References

1. Chen X, Mao SS. Titanium Dioxide Nanomaterials: Synthesis, Properties, Modifications, and Applications. Chemical Reviews. 2007;107(7):2891-959.
2. Sellappan R. Mechanisms of enhanced activity of model TiO2/carbon and TiO2/metal nanocomposite photocatalysts. Chalmers University of Technology; 2013.
3. Carp O. Photoinduced reactivity of titanium dioxide. Progress in Solid State Chemistry. 2004;32(1-2):33-177.
4. Woan K, Pyrgiotakis G, Sigmund W. Photocatalytic Carbon-Nanotube-TiO2Composites. Advanced Materials. 2009;21(21):2233-9.
5. Cong Y, Li X, Qin Y, Dong Z, Yuan G, Cui Z, et al. Carbon-doped TiO2 coating on multiwalled carbon nanotubes with higher visible light photocatalytic activity. Applied Catalysis B: Environmental. 2011;107(1-2):128-34.
6. Di J, Li S, Zhao Z, Huang Y, Jia Y, Zheng H. Biomimetic CNT@ TiO2 composite with enhanced photocatalytic properties. Chemical Engineering Journal. 2015;281:60-8.
7. Yao Y, Li G, Ciston S, Lueptow RM, Gray KA. Photoreactive TiO2/Carbon Nanotube Composites: Synthesis and Reactivity. Environmental Science & Technology. 2008;42(13):4952-7.
8. Eder D, Windle AH. Morphology control of CNT-TiO2 hybrid materials and rutile nanotubes. Journal of Materials Chemistry. 2008;18(17):2036.
9. Serp P, Figueiredo JL, editors. Carbon materials for catalysis. John Wiley & Sons; 2009 Feb 4.
10. Robel I, Bunker BA, Kamat PV. Single-Walled Carbon Nanotube-CdS Nanocomposites as Light-Harvesting Assemblies: Photoinduced Charge-Transfer Interactions. Advanced Materials. 2005;17(20):2458-63.
11. Kamat PV. Harvesting photons with carbon nanotubes. Nano Today. 2006;1(4):20-7.
12. Kongkanand A, Kamat PV. Electron Storage in Single Wall Carbon Nanotubes. Fermi Level Equilibration in Semiconductor–SWCNT Suspensions. ACS Nano. 2007;1(1):13-21.
13. Xu Y-J, Zhuang Y, Fu X. New Insight for Enhanced Photocatalytic Activity of TiO2 by Doping Carbon Nanotubes: A Case Study on Degradation of Benzene and Methyl Orange. The Journal of Physical Chemistry C. 2010;114(6):2669-76.
14. Ząbek P, Eberl J, Kisch H. On the origin of visible light activity in carbon-modified titania. Photochemical & Photobiological Sciences. 2009;8(2):264.
15. Yu H, Quan X, Chen S, Zhao H, Zhang Y. TiO2–carbon nanotube heterojunction arrays with a controllable thickness of TiO2 layer and their first application in photocatalysis. Journal of Photochemistry and Photobiology A: Chemistry. 2008;200(2-3):301-6.
16. Yen C-Y, Lin Y-F, Hung C-H, Tseng Y-H, Ma C-CM, Chang M-C, et al. The effects of synthesis procedures on the morphology and photocatalytic activity of multi-walled carbon nanotubes/ TiO2nanocomposites. Nanotechnology. 2008;19(4):045604.
17. Eder D, Windle AH. Carbon–Inorganic Hybrid Materials: The Carbon-Nanotube/TiO2 Interface. Advanced Materials. 2008;20(9):1787-93.
18. Akhavan O, Azimirad R, Safa S, Larijani MM. Visible light photo-induced antibacterial activity of CNT–doped TiO2 thin films with various CNT contents. Journal of Materials Chemistry. 2010;20(35):7386.
19. Brinker CJ, Scherer GW. Sol-gel science: the physics and chemistry of sol-gel processing. Academic press; 2013 Oct 22.
20. Mamunya Y, Iurzhenko M. Advances in progressive thermoplastic and thermosetting polymers, perspectives and applications. CCUE NASU in IMC NASU; 2012.
21. Williamson GK, Hall WH. X-ray line broadening from filed aluminium and wolfram. Acta Metallurgica. 1953;1(1):22-31.
22. Xie Y, Qian H, Zhong Y, Guo H, Hu Y. Facile Low-Temperature Synthesis of Carbon Nanotube/ Nanohybrids with Enhanced Visible-Light-Driven Photocatalytic Activity. International Journal of Photoenergy. 2012;2012:1-6.
23. Wang W, Serp P, Kalck P, Faria JL. Visible light photodegradation of phenol on MWNT-TiO2 composite catalysts prepared by a modified sol–gel method. Journal of Molecular Catalysis A: Chemical. 2005;235(1-2):194-9.
24. Montero-Ocampo C, Garcia JV, Estrada EA. Comparison of TiO2 and TiO2-CNT as cathode catalyst supports for ORR. Int. J. Electrochem. Sci. 2013 Dec 1;8:12780-800.
25. Zhou W, Zhou Y, Tang S. Formation of TiO2 nano-fiber doped with Gd3+ and its photocatalytic activity. Materials Letters. 2005;59(24-25):3115-8.
26. Sinkó K. Influence of Chemical Conditions on the Nanoporous Structure of Silicate Aerogels. Materials. 2010;3(1):704-40.
27. Niederberger M. Nonaqueous Sol–Gel Routes to Metal Oxide Nanoparticles. Accounts of Chemical Research. 2007;40(9):793-800.
28. Kumar Y, Herrera-Zaldivar M, Olive-Méndez S, Singh F, Mathew X, Agarwal V. Modification of optical and electrical properties of zinc oxide-coated porous silicon nanostructures induced by swift heavy ion. Nanoscale Research Letters. 2012;7(1):366.